ACS OMEGA

http://pubs.acs.org/journal/acsodf

Article

Heat Treatment Improves the Activity and Water Tolerance of Pt/Al_2O_3 Catalysts in Ammonia Catalytic Oxidation

Jianhua Liu, Guangyan Xu,* Qi An, Yingjie Wang, Yunbo Yu, and Hong He

Cite This: *ACS Omega* 2023, 8, 13944−13954

Read Online

ACCESS | Metrics & More | Article Recommendations | Supporting Information

ABSTRACT: Ammonia selective catalytic oxidation (NH_3-SCO) is a commercial technology applied to diesel vehicles to eliminate ammonia leakage. In this study, a series of Pt/Al_2O_3 catalysts were synthesized by an impregnation method, and the state of Pt species was carefully adjusted by heat treatment. These Pt/Al_2O_3 catalysts were further systematically characterized by Brunauer−Emmett−Teller, X-ray diffraction, X-ray photoelectron spectroscopy, X-ray absorption fine structure, UV−vis, H_2-tempertaure-programmed reduction, and NH_3-temperature-programmed desorption. The characterization results showed that dispersed oxidized Pt species were present on conventional Pt/Al_2O_3 samples, while high-temperature treatment induced the aggregation of platinum species to form metallic Pt nanoparticles. The Pt/Al_2O_3 catalysts treated at high temperatures showed superior activity and water tolerance in the NH_3-SCO reaction. Diffuse reflectance infrared Fourier-transform spectroscopy combined with mass spectrometry experiments revealed that the Lewis acid sites were more reactive than the Brønsted acid sites. Moreover, compared to oxidized Pt species, metallic Pt nanoparticles were beneficial for oxygen activation and were less affected by water vapor, thus contributing to the superior activity and water tolerance of Pt/Al-800.

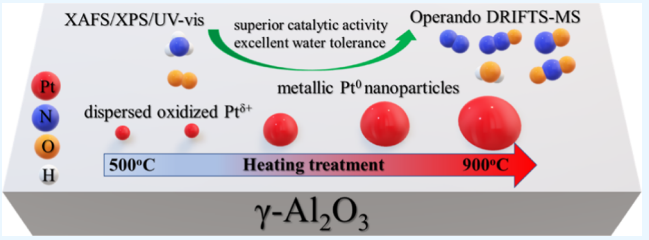

1. INTRODUCTION

Ammonia (NH_3) is a harmful alkaline gas, which can cause serious harm to human health and the ecological environment.[1,2] Vehicle emissions are considered a major source of NH_3 in the urban atmosphere, especially ammonia leakage from diesel vehicles using selective catalytic reduction (SCR) technology.[3−5] Ammonia selective catalytic oxidation (NH_3-SCO) technology is widely recognized as an efficient and environmentally friendly method for NH_3 elimination.[3,6,7] Generally, an ammonia oxidation catalyst (AOC) is expected to completely oxidize NH_3 to harmless N_2 and H_2O at low temperatures.[8,9] Unfortunately, the AOCs with superior low-temperature activity usually will over-oxidize NH_3 to form undesired N_2O and NOx, thus inducing poor N_2 selectivity.[10−12] Hence, investigating the reaction mechanism of NH_3 oxidation is critical for designing highly efficient AOCs.

Until now, various materials have been studied for the NH_3-SCO reaction, including noble metal catalysts (Pt, Ru, Ir, Au, and Rh),[8,13−16] modified zeolite catalysts,[10,17−20] and transition metal oxide catalysts.[21−25] Noble metal catalysts are generally recognized as the most efficient AOCs due to their superior catalytic performance at temperatures below 300 °C.[26−28] In particular, the Pt/Al_2O_3 catalyst was reported to be the most active AOC due to its superior activity and is widely used in practical applications.[29] However, this catalyst still suffers from poor N_2 selectivity on account of the over-oxidation of NH_3 to produce the undesirable byproducts N_2O and NOx.[18,30,31] Generally, the state of active species will significantly affect the activity and selectivity of AOCs during NH_3 oxidation.[32]

There are three main reaction mechanisms for the NH_3-SCO reaction which have been reported in different catalyst systems: the imide (−NH) mechanism,[33−35] the hydrazine (N_2H_4) mechanism,[24,29] and the internal SCR (i-SCR) mechanism.[19,36,37] As one of the most active noble metal catalysts, the reaction mechanism of Pt catalysts varies with the state of Pt, which is regulated by many factors. Mieher and Ho[38] studied the mechanism of NH_3 oxidation on Pt(111), and they proposed that the reaction followed the imide mechanism. However, different supports will also affect the reaction process on Pt-based catalysts. Chen *et al.*[39] compared the reaction mechanisms of NH_3-SCO on Pt/Al_2O_3 and Pt/$CeZrO_2$, and they found that metallic Pt promoted the deep dehydrogenation of NH_3 and that the reaction obeyed the imide mechanism on Pt/Al_2O_3. By contrast, HNO and N_2H_4 were observed on Pt/$CeZrO_2$ during NH_3 oxidation, indicating the coexistence of the imide mechanism and the hydrazine mechanism. Clearly, the state of Pt species

Received: January 18, 2023
Accepted: March 24, 2023
Published: April 6, 2023

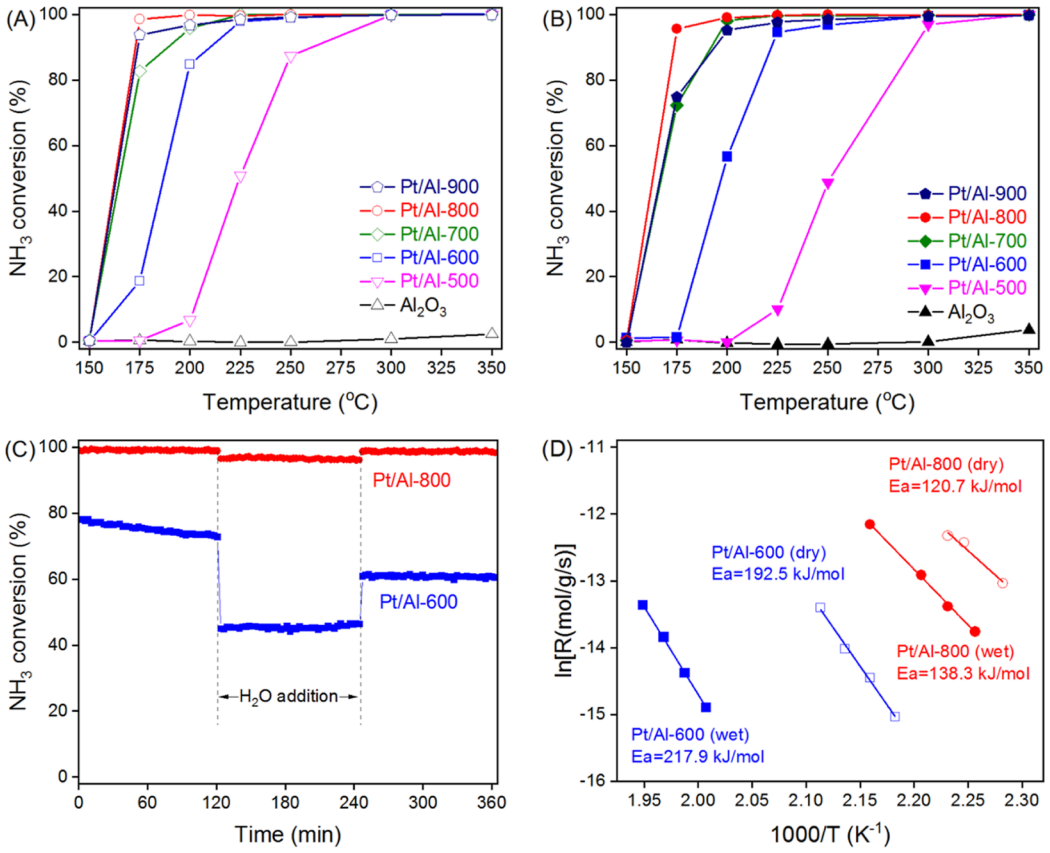

Figure 1. NH_3 conversion in the NH_3-SCO reaction over Pt/Al_2O_3 catalysts in the absence (A) and presence (B) of water vapor. Effect of H_2O addition on NH_3 conversion over Pt/Al_2O_3 catalysts at 200 °C (C). Arrhenius plots of NH_3 conversion over Pt/Al_2O_3 under different conditions (D). Feed composition: 550 ppm NH_3, 5% O_2, and 5% H_2O (when added) in the N_2 balance.

significantly affects the reaction pathway of ammonia oxidation on Pt-based catalysts.

Herein, a series of Pt/Al_2O_3 catalysts were prepared, and the state of Pt species was carefully adjusted by heat treatment. Afterward, these samples were systematically characterized by N_2 adsorption, X-ray diffraction (XRD), high-resolution transmission electron microscopy (HR-TEM), ultraviolet−visible spectrophotometry (UV−vis), X-ray photoelectron spectroscopy (XPS), X-ray absorption fine structure (XAFS), NH_3 temperature-programmed desorption (NH_3-TPD), and H_2 temperature-programmed reduction (H_2-TPR). Moreover, the reaction mechanism of NH_3 oxidation on these Pt/Al_2O_3 catalysts was investigated by kinetic studies and operando diffuse reflectance infrared Fourier-transform spectroscopy combined with mass spectrometry (DRIFTS-MS). This study provides new understanding on the mechanism of NH_3 oxidation over supported Pt catalysts and offers some advice for designing high-efficiency AOCs.

2. EXPERIMENTAL SECTION

A series of Pt/Al_2O_3 catalysts with 0.5 wt % Pt loading were prepared by an impregnation method using boehmite (Sasol, SB-1) as the support, which was pre-calcined at 800 °C for 6 h.[40,41] Afterward, these Pt/Al_2O_3 catalysts were calcined in a muffle furnace at different temperatures for 3 h and were further denoted as Pt/Al-X, where X refers to the calcination temperature. The catalytic testing was performed on a fixed-bed flow reactor connected to an infrared spectrometer (Nicolet iS 50). Then, these Pt/Al_2O_3 catalysts were systematically characterized by various techniques, and detailed information on catalyst synthesis, activity testing, and characterization can be found in the Supporting Information.

3. RESULTS

Figure 1 shows the catalytic performance of Pt/Al_2O_3 in NH_3 oxidation in the absence and presence of water vapor. Pure Al_2O_3 was entirely inactive for NH_3 oxidation, achieving negligible NH_3 conversion throughout the activity test, regardless of the absence or presence of water vapor. In contrast, Pt/Al-500 exhibited superior catalytic activity for NH_3 oxidation at temperatures below 250 °C. Notably, increasing the calcination temperature significantly enhanced the low-temperature activity of Pt/Al_2O_3 catalysts for NH_3 oxidation. Specifically, Pt/Al-500 achieved an NH_3 conversion of 87% at 250 °C, while Pt/Al-600 and Pt/Al-700 obtained 85 and 83% NH_3 conversion at 200 and 175 °C, respectively. Moreover, the Pt/Al-800 catalyst almost completely oxidized NH_3 (98.6%) at the low temperature of 175 °C, while further increasing the calcination temperature resulted in a slight decrease in the catalytic activity of Pt/Al-900. Unfortunately, the N_2 selectivity gradually decreased from ∼85% (175 °C) to ∼20% (350 °C) as the reaction temperature increased (Figure S1).

In the presence of H_2O (Figure 1B), the catalytic activity of the Pt/Al_2O_3 catalysts was suppressed to some extent, especially in the samples calcined at low temperatures. For example, on the Pt/Al-600 catalyst, the NH_3 conversion at 200 °C was decreased to 56.7% in the presence of H_2O, which was

https://doi.org/10.1021/acsomega.3c00381
ACS Omega 2023, 8, 13944−13954

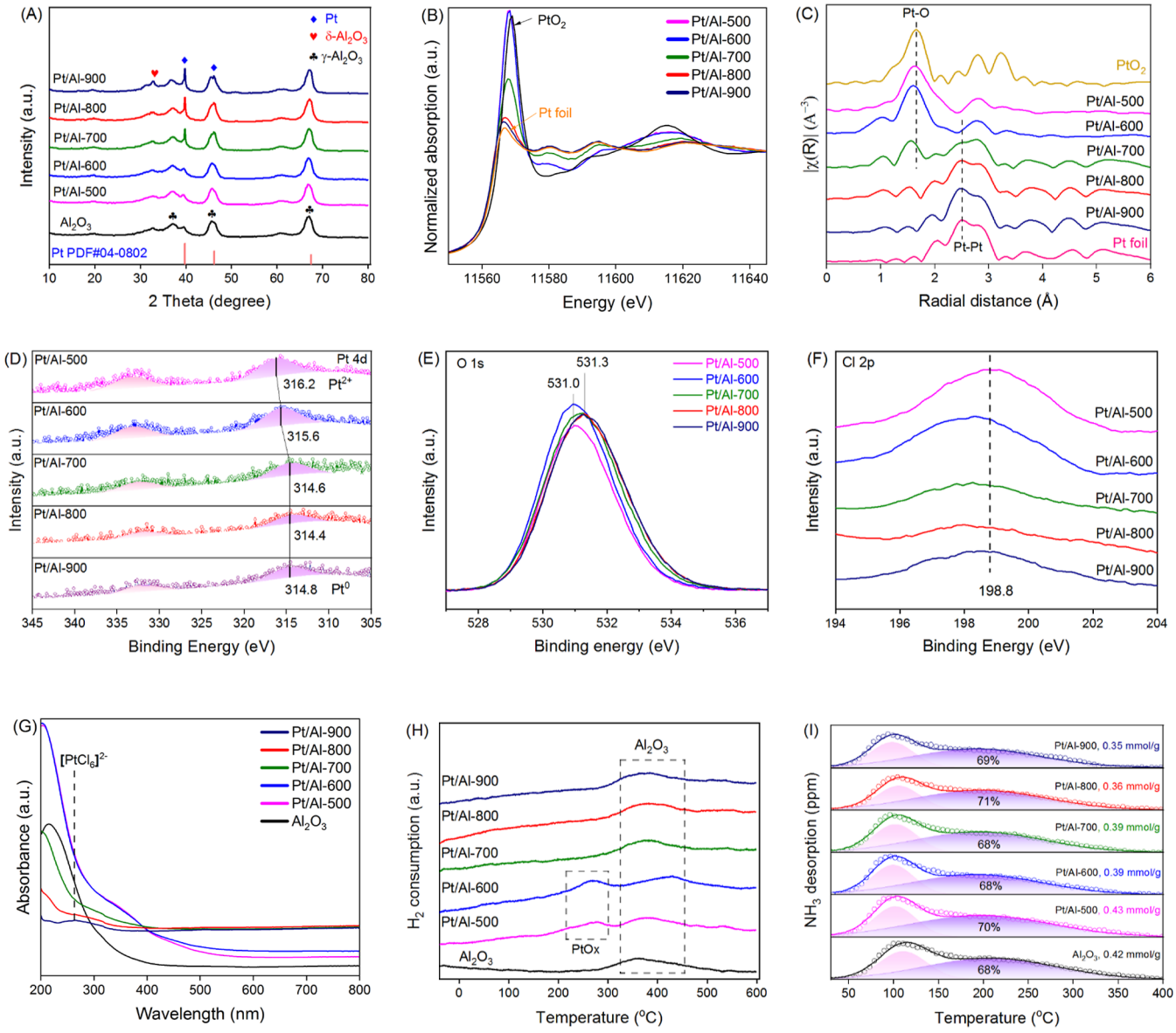

Figure 2. XRD patterns (A), normalized Pt-L_{III} XANES spectra (B), k^2-weighted EXAFS spectra (C), Pt 4d XPS spectra (D), O 1s XPS spectra (E), Cl 2p XPS spectra (F), DR-UV−vis spectra (G), H_2-TPR profiles (H), and NH_3-TPD profiles (I) of Pt/Al_2O_3 catalysts.

significantly lower than that without water vapor (85%). In contrast, Pt/Al-800 was hardly affected by water vapor, achieving an NH_3 conversion of 95.6% at 175 °C, and the N_2 selectivity was similar to that in the absence of water vapor. Compared to related catalysts reported in the previous literature,[8−10,31,39] the obtained Pt/Al-800 catalyst proved to be one of the most active catalysts (Table S1). The reaction products of NH_3 oxidation on these Pt/Al_2O_3 catalysts are shown in Figure S2. On Pt/Al-500, the formation of N_2 and N_2O exhibited a similar trend, achieving a maximum value at about 300 °C. Notably, the temperature for maximum N_2 generation gradually dropped on Pt/Al_2O_3 catalysts pretreated at higher temperatures. Instead, the temperature for maximum N_2O formation remained stable at 250 °C over various Pt/Al_2O_3 catalysts. This indicated that the reaction mechanisms for the generation of N_2 and N_2O were slightly different. Besides, even in the presence of water vapor at a high gas hourly space velocity of 400,000 h^{-1}, the Pt/Al-800 catalyst still showed excellent catalytic performance (Figure S3), revealing its superior ability in practical applications.

A step-response experiment was further performed to investigate the effect of water vapor on these Pt/Al_2O_3 catalysts (Figure 1C). On Pt/Al-600, the NH_3 conversion suddenly decreased from 73 to 44% on the introduction of H_2O, while it could not be restored entirely (61%) after the removal of water vapor, revealing that the influence of H_2O on this sample was irreversible. On the contrary, the Pt/Al-800 catalyst was hardly affected by water addition, achieving >96% NH_3 conversion regardless of the presence of water vapor and exhibiting superior water tolerance. To further investigate the difference between these Pt/Al_2O_3 catalysts, kinetic measurements were performed, and Arrhenius plots are shown in Figure 1D. In the absence of H_2O, the apparent activation energy (Ea) on Pt/Al-800 (120.7 kJ/mol) was significantly lower than that on Pt/Al-600 (192.5 kJ/mol). The introduction of water vapor slightly increased the Ea on both samples, while the Ea on Pt/Al-800 (138.3 kJ/mol) was still

https://doi.org/10.1021/acsomega.3c00381
ACS Omega 2023, 8, 13944−13954

remarkably lower than that on Pt/Al-600 (217.9 kJ/mol). Clearly, the activation energy for NH_3 oxidation on Pt/Al-800 was much lower than that on Pt/Al-600 despite the presence of H_2O in the reaction system. Based on the above tests, it was concluded that the Pt/Al_2O_3 samples pretreated at high temperatures showed superior low-temperature activity and water tolerance in the NH_3-SCO reaction.

These Pt/Al_2O_3 catalysts were further systematically characterized using various techniques (Figure 2). The N_2 adsorption results show that Al_2O_3 had a Brunauer−Emmett−Teller-specific surface area of 167.9 m^2/g, and the introduction of platinum species hardly affected the surface properties of the Pt/Al_2O_3 catalysts (Table S2). In contrast, high-temperature treatment induced a slight decrease in the specific surface area of Pt/Al_2O_3 samples, especially on Pt/Al-900 (139.3 m^2/g), possibly caused by the sintering of the Al_2O_3 support.[42] XRD patterns showed that only the γ-Al_2O_3 crystal phase (2θ = 67, 45.6, and 37.2°) was observed on the Pt/Al_2O_3 catalysts calcined at low temperatures (Figure 2A), revealing the good dispersion of platinum species. In contrast, metallic Pt species (2θ = 46.2 and 39.7°) emerged on the Pt/Al_2O_3 samples pretreated at high temperatures. Moreover, a weak diffraction peak (2θ = 32.8°) due to δ-Al_2O_3 appeared in the pattern of Pt/Al-900, possibly due to the transition of γ-Al_2O_3 during heat treatment, consistent with the surface properties.[43] HR-TEM images also confirmed the existence of Pt nanoparticles on the Pt/Al_2O_3 catalysts pretreated at high temperatures (Figure S4). Besides, the morphology of the Al_2O_3 carrier did not appear to be affected by heat treatment, and the effect of the carrier morphology was not further discussed in the present work.

X-ray absorption near-edge structure spectra showed that the white lines of the $Pt\text{-}_{LIII}$ edge of Pt/Al-500 and Pt/Al-600 were close to those of the PtO_2 reference, while the white lines of Pt/Al-800 and Pt/Al-900 were near those of the Pt foil (Figure 2B). Extended XAFS (EXAFS) spectra showed that the peak (1.8 Å) due to the first shell of Pt−O scattering was found on Pt/Al-500 and Pt/Al-600, while the signal for Pt−Pt scattering was not observed for these samples (Figure 2C).[32] In contrast, only the peak (2.5 Å) due to the first shell of Pt−Pt scattering was found on Pt/Al-800 and Pt/Al-900.[44] These results indicated that dispersed oxidized Pt species were present on Pt/Al-500 and Pt/Al-600, while metallic Pt nanoparticles were present on Pt/Al_2O_3 catalysts pretreated at high temperatures.

The XPS spectra showed that the binding energies of Pt $4d_{5/2}$ on Pt/Al-500 (316.2 eV) and Pt/Al-600 (315.6 eV) were significantly higher than those on Pt/Al-800 (314.4 eV) and Pt/Al-900 (314.8 eV), indicating that more electron-rich Pt species were present on the Pt/Al_2O_3 catalysts pretreated at high temperatures (Figure 2D).[10,45] Moreover, the binding energy of O 1s on Pt/Al-500 and Pt/Al-600 (531.0 eV) was slightly lower than that on Pt/Al-800 and Pt/Al-900 (531.3 eV), suggesting the presence of electron-rich O species on the former two samples (Figure 2E). This was consistent with the XAFS results showing that oxidized Pt species were present on Pt/Al-500 and Pt/Al-600, while metallic Pt species were present on Pt/Al-800 and Pt/Al-900. Besides, the XPS spectra also showed that a minor peak (198.8 eV) due to the Cl 2p orbital was observed on these Pt/Al_2O_3 catalysts, which was attributed to residual Cl^- from the preparation process. According to the previous literature,[32,46] the presence of residual Cl^- on Pt/Al_2O_3 catalysts could enhance the sinter resistance of Pt species during calcination, thus resulting in the highly dispersed oxidized Pt species on Pt/Al-500 and Pt/Al-600. In contrast, high-temperature pretreatment could remove the residual Cl^- species and promote the decomposition and aggregation of oxidized Pt species to form metallic Pt nanoparticles on Pt/Al-800 and Pt/Al-900. UV−vis analysis further confirmed the presence of $[PtCl_6]^{2-}$ species (263 nm) on Pt/Al-500 and Pt/Al-600,[47−49] while they could not be observed on the samples pretreated at high temperatures (Figure 2G).

A H_2-TPR experiment was further performed to study the redox properties of the Pt/Al_2O_3 catalysts (Figure 2H). A minor H_2 consumption peak at around 350−450 °C was observed for Al_2O_3, attributed to the reduction of surface oxygen species.[50,51] Besides, another peak at ∼ 250 °C was observed for Pt/Al-500 and Pt/Al-600, which was assigned to the reduction of oxidized PtOx species.[52] The H_2 consumption due to the reduction of PtOx on Pt/Al-500 and Pt/Al-600 was 17.2 and 10.5 μmol/g, respectively. However, the H_2 consumption should be between 25.6 and 51.2 μmol/g assuming that all the PtOx species (PtO and PtO_2) on the Pt/Al_2O_3 catalysts were reduced completely.[39] Hence, it suggested that a significant amount of PtOx on Pt/Al-500 and Pt/Al-600 could not be reduced under the H_2-TPR condition, which might be due to the effect of the residual Cl^- species.[32] In contrast, no H_2 consumption due to Pt species was observed on the Pt/Al_2O_3 samples pretreated at high temperatures. An NH_3-TPD experiment was conducted to further evaluate the acid properties of these Pt/Al_2O_3 catalysts (Figure 2I). The TPD profile could be deconvoluted into two peaks: the peak at low temperature (∼100 °C) was attributed to the desorption of weakly adsorbed NH_3, and the broad peak at 150−300 °C was assigned to NH_3 bonded to strong acid sites.[32] The amount of NH_3 desorption on Al_2O_3 was 0.42 mmol/g, and the introduction of Pt species only slightly increased the number of acid sites on Pt/Al-500 (0.43 mmol/g). High-temperature calcination induced a slight decrease in the number of acid sites on Pt/Al-800 (0.36 mmol/g) and Pt/Al-900 (0.35 mmol/g), possibly due to the decrease in the specific surface area on these samples.

The reaction mechanism of NH_3 oxidation on Pt/Al_2O_3 catalysts was further investigated by an operando DRIFTS-MS experiment. DRIFTS spectra of NH_3 adsorption showed that several peaks could be observed on Al_2O_3 (Figure 3),

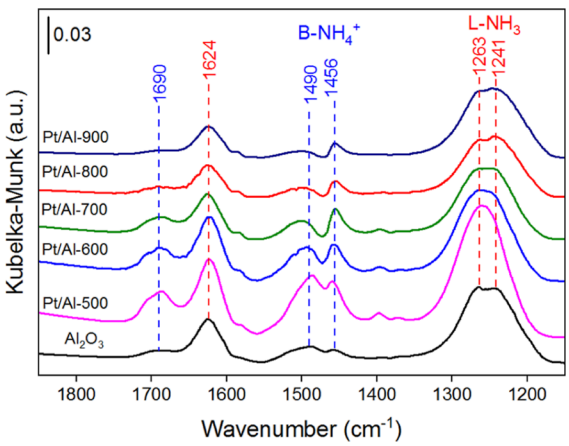

Figure 3. *In situ* DRIFTS spectra of NH_3 adsorption on Pt/Al_2O_3 catalysts at 100 °C. Feed composition: 1000 ppm NH_3 in Ar balance.

https://doi.org/10.1021/acsomega.3c00381
ACS Omega 2023, 8, 13944−13954

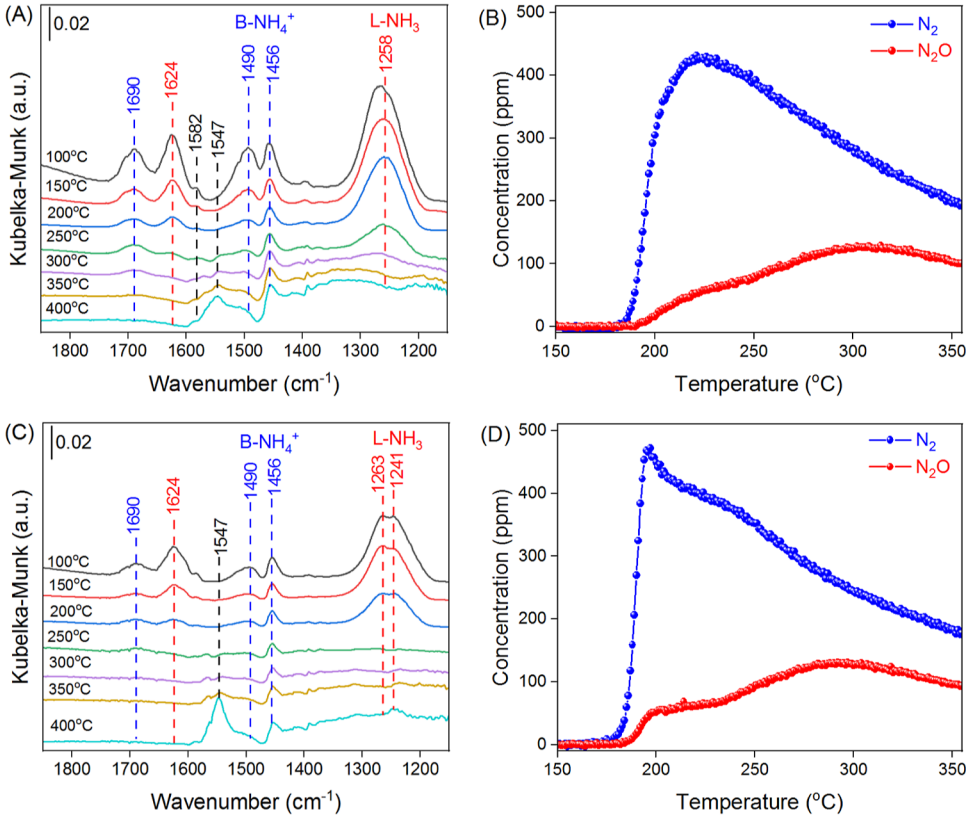

Figure 4. Operando DRIFTS-MS experiment of the NH_3-SCO reaction: DRIFTS spectra of Pt/Al-600 (A) and Pt/Al-800 (C) and corresponding gaseous products on Pt/Al-600 (B) and Pt/Al-800 (D). Feed composition: 1000 ppm NH_3 and 5% O_2 in Ar balance.

attributed to the vibrations of NH_3 coordinated on Lewis acid sites (1241, 1263, and 1624 cm^{-1}) and NH_4^+ bonded to Brønsted acid sites (1456 and 1490 cm^{-1}).[35,53−55] After impregnation with platinum species, the number of adsorbed NH_3 species on the Pt/Al_2O_3 catalysts was significantly increased, including those on both Lewis acid sites (1241, 1263, and 1624 cm^{-1}) and Brønsted acid sites (1456, 1490, and 1690 cm^{-1}). The increase might be related to Pt species and hydroxyl group formation due to chlorine species. After heat treatment, the number of Brønsted acid sites on Pt/Al-800 and Pt/Al-900 was remarkably decreased, and the intensities of the peaks due to Lewis acid sites were equal to those of Al_2O_3. Therefore, it was speculated that the Lewis acid sites on the Pt/Al_2O_3 catalysts were mainly composed of Al sites, and the Brønsted acid sites were related to the surface hydroxyl groups bonded to oxidized Pt species and chlorine species.[56−60] The result was consistent with NH_3-TPD analysis, while the difference might be due to the different adsorption temperatures and experimental setup.

A DRIFTS-MS experiment of the temperature-programmed surface reaction was conducted on these Pt/Al_2O_3 catalysts (Figure 4). After pretreatment, the catalysts were exposed to NH_3/O_2 at 100 °C for 120 min, followed by heating to 400 °C (2 °C/min). On Pt/Al-600, a large amount of adsorbed NH_3 on both Lewis acid sites and Brønsted acid sites was observed at 100 °C, whereas neither N_2 nor N_2O was produced (Figure 4A,B). As the reaction temperature gradually ramped up to 225 °C, a large amount of gaseous N_2 was produced, accompanied by a rapid decrease in adsorbed NH_3 species, especially those on the Lewis acid sites. Further increasing the reaction temperature induced a slight increase in N_2O formation and a gradual decrease in N_2 generation. NH_3 adsorbed on Lewis acid sites vanished at temperatures above 300 °C, while a certain amount of NH_4^+ bonded to Brønsted acid sites (1456 cm^{-1}) was still observed even at a high temperature of 400 °C. Moreover, nitrate species (1547 and 1582 cm^{-1}) gradually emerged at temperatures above 300 °C, which possibly contributed to the formation of gaseous NOx.[61−63]

On the Pt/Al-800 sample (Figure 4C,D), NH_3 oxidation was slightly enhanced at lower temperatures, achieving a maximum production of N_2 at 200, 25 °C lower than the corresponding temperature on Pt/Al-600. Similarly, N_2 formation gradually decreased as the temperature further increased to 350 °C, while N_2O generation was enhanced in this process. Generally, the change in the intensity of peaks due to Lewis acid sites (1241 and 1263 cm^{-1}) was consistent with the light-off curve of N_2 formation, indicating the critical role of Lewis acid sites in this reaction. In contrast, NH_4^+ bonded to Brønsted acid sites (1456 cm^{-1}) remained stable even at high temperatures. Moreover, characteristic peaks (2237 and 2210 cm^{-1}) due to adsorbed N_2O were also observed on these samples at temperatures above 250 °C (Figure S5), consistent with the formation of gaseous N_2O.[64,65] Experiments on other Pt/Al_2O_3 catalysts showed similar phenomena and further confirmed the critical role of Lewis acid sites in this reaction (Figure S6).

To further investigate the reactivity of different acid sites, a step-response experiment was performed on these Pt/Al_2O_3 catalysts at different temperatures. Pure Al_2O_3 was inactive for NH_3 oxidation at 200 °C (Figure 1), and the adsorbed NH_3 species on Al_2O_3 hardly reacted with gaseous O_2, with negligible N_2 produced (Figure S7A). Incidentally, the gaseous O_2 employed contained low concentrations of N_2 and CO_2

https://doi.org/10.1021/acsomega.3c00381
ACS Omega 2023, 8, 13944−13954

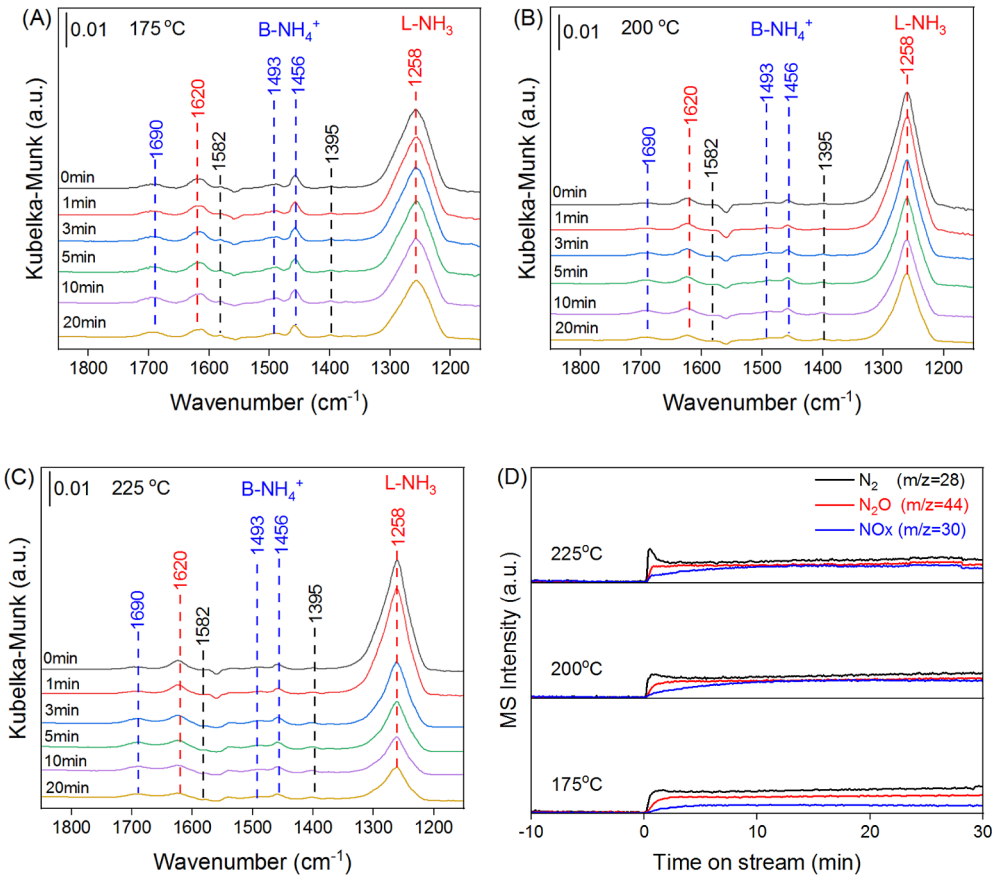

Figure 5. Reactivity of adsorbed NH_3 toward O_2 on Pt/Al-600 at 175 (A), 200 (B), and 225 °C (C) and corresponding gaseous products (D). Feed composition: 1000 ppm NH_3 and 5% O_2 in Ar balance.

(m/z = 44), which were brought into the reaction gas when O_2 was introduced (Figure S7B). On the Pt/Al-600 catalyst, the adsorbed NH_3 species were also found to hardly react with O_2 to form surface intermediates or gaseous products at the low temperatures of 175 and 200 °C (Figure 5A,B, respectively). As the reaction ramped up to 225 °C, NH_3 adsorbed on the Lewis acid sites (1258 cm^{-1}) could slowly react with gaseous O_2 to generate a small amount of N_2 in the first few minutes (Figure 5C). During the above-mentioned processes, NH_4^+ bonded to Brønsted acid sites was inactive toward O_2, and the associated peak (1456 cm^{-1}) had low intensity.

On Pt/Al-800, the adsorbed NH_3 species on the Lewis acid sites (1241 and 1263 cm^{-1}) showed high reactivity toward gaseous O_2 even at the low temperature of 175 °C, generating a certain amount of N_2 in the first few minutes (Figure 6A). The reaction was remarkably enhanced as the temperature increased to 200 and 225 °C, with more N_2 produced on exposure to O_2. Similar to Pt/Al-600, a small amount of NH_4^+ on Brønsted acid sites (1456 and 1493 cm^{-1}) was observed and showed low reactivity in this reaction. Moreover, Pt/Al-500 showed performance similar to that of Pt/Al-600, while Pt/Al-700 and Pt/Al-900 showed performance close to that of Pt/Al-800 (Figure S8).

To better evaluate the reactivity of adsorbed NH_3 species on the Pt/Al_2O_3 catalysts, another experiment was performed on these samples (Figures 7 and S9). The samples were pre-exposed to NH_3/Ar at 200 °C for 30 min and then further exposed to O_2/NH_3/Ar for 30 min. On Pt/Al-600, the introduction of O_2 hardly affected the adsorption of NH_3 species and induced a negligible increase in N_2 formation (Figure 7A). This indicated that the activation of O_2 and its further reaction with adsorbed NH_3 were the rate-determining step on this sample at 200 °C. On Pt/Al-800, by contrast, the adsorbed NH_3 species, especially those on the Lewis acid sites (1258 and 1220 cm^{-1}), rapidly reacted with O_2 to generate a large amount of N_2 (Figure 7B). Notably, the amount of adsorbed NH_3 on Lewis acid sites (1258 and 1220 cm^{-1}) was significantly decreased, revealing that O_2 activation and its further reaction were faster than NH_3 adsorption under current conditions, making NH_3 adsorption the rate-determining step on this sample. The same experiment was conducted on other Pt/Al_2O_3 catalysts (Figure S9), and the result further confirmed that O_2 activation was inefficient on the Pt/Al_2O_3 catalysts calcined at low temperatures. In contrast, O_2 activation was enhanced, and NH_3 adsorption became the rate-determining step on the Pt/Al_2O_3 catalysts pretreated at high temperatures.

4. DISCUSSION

In the present work, the state of Pt species on the Pt/Al_2O_3 catalysts was carefully regulated by adjusting the heat treatment. EXAFS and XPS spectra indicated that the platinum species were mainly present as dispersed oxidized Pt species on the Pt/Al_2O_3 catalysts pretreated at lower temperatures. On Pt/Al-800 and Pt/Al-900, by contrast, these oxidized Pt species gradually decomposed and converted to metallic Pt nanoparticles during heat treatment. Besides, a certain amount of Lewis acid sites was observed on the Al_2O_3 support, while

https://doi.org/10.1021/acsomega.3c00381
ACS Omega 2023, 8, 13944−13954

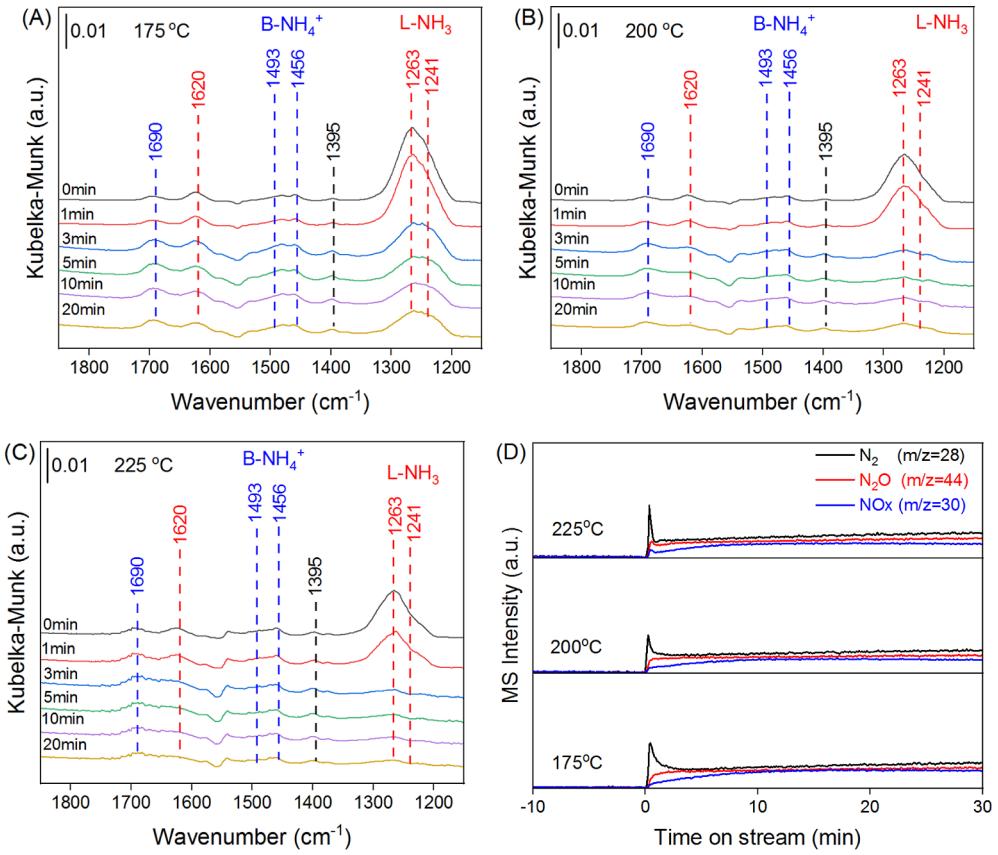

Figure 6. Reactivity of adsorbed NH_3 toward O_2 on Pt/Al-800 at 175 (A), 200 (B), and 225 °C (C) and corresponding gaseous products (D). Feed composition: 1000 ppm NH_3 and 5% O_2 in Ar balance.

the introduction of Pt species significantly increased the number of Brønsted acid sites on Pt/Al-500 and Pt/Al-600. In contrast, these Brønsted acid sites on the Pt/Al_2O_3 catalysts gradually vanished after heat treatment, possibly due to the elimination of chlorine species and the formation of metallic Pt nanoparticles.

During the NH_3-SCO reaction, the Pt/Al_2O_3 catalysts pretreated at different temperatures exhibited distinctly different catalytic performances. Specifically, the low-temperature activity of the series of Pt/Al_2O_3 catalysts was gradually improved as the calcination temperature increased. In particular, Pt/Al-800 showed extremely high activity for NH_3 catalytic oxidation at the reaction temperature of 175 °C, regardless of the absence or presence of water vapor. Despite the superior activity, the N_2 selectivity on these Pt-based catalysts should be further improved. Previous studies have shown that doping of transition metals (Cu, Fe, and V) can improve the N_2 selectivity of Pt-based catalysts but at the expense of a decrease in the low-temperature activity.[8,10,18,45] Besides, bi-functional catalysts with dual layers (Pt/Al_2O_3 + Cu/SSZ-13) or a core−shell structure (Pt/Al_2O_3@Cu/ZSM-5) proved to be effective in the NH_3-SCO reaction with high N_2 selectivity.[11,30,31,66] Recently, Zhang *et al.*[25] proposed a fast i-SCR mechanism on a novel $CuOx/Al_2O_3$-H catalyst, which showed high activity and N_2 selectivity in the NH_3-SCO reaction.

Generally, NH_3-SCO involves two steps, including NH_3 adsorption and O_2 activation. In the present work, the Al_2O_3 support, with a high specific surface area, provided abundant acid sites for NH_3 adsorption, and Pt species were responsible for O_2 activation. The NH_3-TPD profiles and DRIFTS spectra showed that Al_2O_3 mainly provided Al Lewis acid sites for NH_3 adsorption. Besides, a certain amount of adsorbed NH_3 on Brønsted acid sites was also observed on Pt/Al-500 and Pt/Al-600, which was unstable and gradually desorbed as the temperature increased. Instead, the adsorbed NH_3 on Pt/Al-800 and Pt/Al-900 was similar to that on the Al_2O_3 support. An operando DRIFTS-MS experiment further confirmed that NH_3 adsorbed on Lewis acid sites was more reactive than that on Brønsted acid sites. Hence, the Lewis acid sites (mainly the Al sites) play an important role in the NH_3-SCO reaction over Pt/Al_2O_3 catalysts.

As mentioned above, heat treatment of the Pt/Al_2O_3 catalysts induced the transformation of oxidized Pt species to metallic Pt nanoparticles, the latter of which possibly showed better ability for O_2 activation. Specifically, EXAFS spectra showed that only oxidized Pt species could be observed on Pt/Al-500 and Pt/Al-600. Instead, both oxidized and metallic Pt species were observed on Pt/Al-700. Consequently, their low-temperature activity was gradually improved, with Pt/Al-700 showing the best performance among them. Notably, on Pt/Al-800 and Pt/Al-900, only metallic Pt species were observed, and these samples exhibited superior activity for NH_3 oxidation at the low temperature of 175 °C. It has been reported that metallic Pt(111) was beneficial for oxygen dissociation to form atomic oxygen species, which further promoted the dehydrogenation of ammonia.[39,67] This suggested that metallic Pt nanoparticles were beneficial for the activation of gaseous O_2, which further participated in NH_3 dehydrogenation and transformation. Instead, oxidized Pt

https://doi.org/10.1021/acsomega.3c00381
ACS Omega 2023, 8, 13944−13954

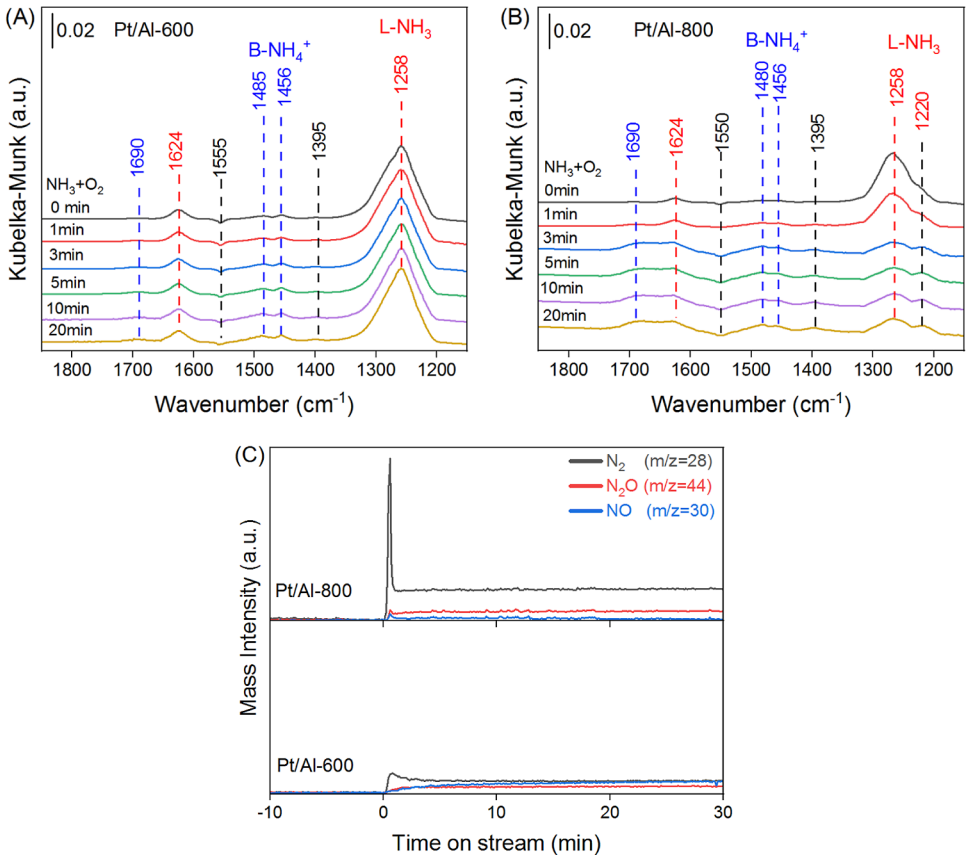

Figure 7. Reactivity of pre-adsorbed NH_3 with O_2 over Pt/Al-600 (A) and Pt/Al-800 (B) at 200 °C and corresponding gaseous products (C). The catalysts were exposed to NH_3 and NH_3 + O_2 successively. Feed composition: 1000 ppm NH_3 and 5% O_2 in Ar balance.

species were inefficient for O_2 activation at low temperatures, and the oxygen species in the oxidized Pt nanoparticles may have participated in the reaction at high temperatures. According to the reaction products (Figure S2), it was speculated that metallic Pt nanoparticles were responsible for N_2 generation, especially at low temperatures. In contrast, the rapid activation of gaseous O_2 on Pt nanoparticles at high temperatures might increase the concentration of surface oxygen species, which further induced the generation of N_2O and NOx.

Based on the above discussion, the reaction mechanism of NH_3-SCO over Pt/Al_2O_3 was proposed. The first step was the activation and dissociation of oxygen on metallic Pt nanoparticles to generate reactive atomic oxygen (eq 1). Then, NH_3 adsorbed on Lewis acid sites reacted with the reactive atomic oxygen to produce $-NH_2$ and $-NH$ intermediates (eqs 2 and 3).[35] Afterward, $-NH$ further reacted with atomic oxygen to form $-HNO$ species, which reacted with $-NH$ species to produce N_2 and H_2O (eqs 4 and 5), and N_2O was also produced (eq 6). At high temperatures, the activation and dissociation of oxygen were greatly enhanced, and $-NH$ species could dehydrogenate deeply to produce atomic N species (eq 7), which further reacted with atomic oxygen to generate NO and NO_2 (eqs 8 and 9).

$$Pt^0 + O_2 \rightarrow Pt^0{-}O_2 \rightarrow Pt^0 + 2O^* \quad (1)$$

$$M{-}NH_3 + O^* \rightarrow M{-}NH_2 + {-}OH \quad (2)$$

$$M{-}NH_2 + O^* \rightarrow M{-}NH + {-}OH \quad (3)$$

$$M{-}NH + O^* \rightarrow M{-}HNO \quad (4)$$

$$M{-}NH + M{-}HNO \rightarrow 2M + N_2 + H_2O \quad (5)$$

$$M{-}HNO + M{-}HNO \rightarrow 2M + N_2O + H_2O \quad (6)$$

$$M{-}NH + O^* \rightarrow M{-}N + {-}OH \quad (7)$$

$$M{-}N + O^* \rightarrow M{-}NO \rightarrow M + NO \quad (8)$$

$$M{-}NO + O^* \rightarrow M + NO_2 \quad (9)$$

Generally, it has been widely reported that water vapor will suppress the reaction of NH_3-SCR and NH_3-SCO due to the competitive adsorption of H_2O and NH_3 for the same adsorption sites.[20] Moreover, the presence of water vapor will also moisten the catalyst surface and change the catalysts' properties, such as inducing the transformation of Lewis acid sites to Brønsted acid sites.[68] In the present work, the Brønsted acid sites were less reactive than the Lewis acid sites. Hence, the interconversion of acid sites caused by water vapor would not benefit the NH_3-SCO reaction. Besides, H_2O could also moisten oxidized Pt species to produce hydrated platinum species, thus affecting the activation and dissociation of O_2, finally resulting in an inferior activity and water tolerance of Pt/Al-600 during the NH_3-SCO reaction.[69,70] Overall, metallic Pt nanoparticles seem less affected by water vapor, and the Pt/Al-800 catalyst shows excellent water tolerance during NH_3 oxidation.

https://doi.org/10.1021/acsomega.3c00381
ACS Omega 2023, 8, 13944−13954

5. CONCLUSIONS

A series of Pt/Al_2O_3 catalysts were synthesized, and the state of Pt species was carefully regulated by heat treatment, and these catalysts were further applied in the NH_3-SCO reaction. On conventional Pt/Al_2O_3 catalysts, the platinum species were mainly present as dispersed oxidized Pt species, which were inefficient for oxygen activation at low temperatures, thus resulting in poor catalytic performance for Pt/Al-500 and Pt/Al-600 in ammonia oxidation. Instead, high-temperature treatment of Pt/Al_2O_3 catalysts induced the aggregation of platinum species to form metallic Pt nanoparticles on Pt/Al-800. DRIFTS-MS experiments revealed that the Lewis acid sites were more reactive than the Brønsted acid sites. Moreover, compared to oxidized Pt species, metallic Pt nanoparticles were beneficial for oxygen activation and less affected by water vapor, thus contributing to the superior activity and water tolerance of Pt/Al-800.

■ ASSOCIATED CONTENT

Supporting Information

The Supporting Information is available free of charge at https://pubs.acs.org/doi/10.1021/acsomega.3c00381.

Experimental section, N_2 selectivity, gaseous product concentration, structural parameters of the Pt/Al_2O_3 catalysts, HR-TEM images, and operando DRIFTS-MS experiment of Pt/Al_2O_3 (PDF)

■ AUTHOR INFORMATION

Corresponding Author

Guangyan Xu − *State Key Joint Laboratory of Environment Simulation and Pollution Control, Research Center for Eco-Environmental Sciences, Chinese Academy of Sciences, Beijing 100085, China;* orcid.org/0000-0002-4275-7517; Email: gyxu@rcees.ac.cn

Authors

Jianhua Liu − *School of Rare Earths, University of Science and Technology of China, Hefei 230026, China; Ganjiang Innovation Academy, Chinese Academy of Sciences, Ganzhou 341000, China*

Qi An − *School of Rare Earths, University of Science and Technology of China, Hefei 230026, China; Ganjiang Innovation Academy, Chinese Academy of Sciences, Ganzhou 341000, China*

Yingjie Wang − *School of Rare Earths, University of Science and Technology of China, Hefei 230026, China; Ganjiang Innovation Academy, Chinese Academy of Sciences, Ganzhou 341000, China*

Yunbo Yu − *School of Rare Earths, University of Science and Technology of China, Hefei 230026, China; Ganjiang Innovation Academy, Chinese Academy of Sciences, Ganzhou 341000, China; State Key Joint Laboratory of Environment Simulation and Pollution Control, Research Center for Eco-Environmental Sciences, Chinese Academy of Sciences, Beijing 100085, China;* orcid.org/0000-0003-2935-0955

Hong He − *School of Rare Earths, University of Science and Technology of China, Hefei 230026, China; Ganjiang Innovation Academy, Chinese Academy of Sciences, Ganzhou 341000, China; State Key Joint Laboratory of Environment Simulation and Pollution Control, Research Center for Eco-Environmental Sciences, Chinese Academy of Sciences, Beijing 100085, China;* orcid.org/0000-0001-8476-8217

Complete contact information is available at: https://pubs.acs.org/10.1021/acsomega.3c00381

Author Contributions

The manuscript was written through the contributions of all authors. All authors have approved the final version of the manuscript.

Notes

The authors declare no competing financial interest.

■ ACKNOWLEDGMENTS

The authors acknowledge the National Key R&D Program of China (2022YFC3704400), the National Natural Science Foundation of China (22276203 and U20B6004), and the project of eco-environmental technology for carbon neutrality (RCEES-TDZ-2021-6).

■ REFERENCES

(1) Jankowska, A.; Kowalczyk, A.; Rutkowska, M.; Michalik, M.; Chmielarz, L. Catalytic Performance of Bimetallic Systems (Cu-Fe, Cu-Mn, Fe-Mn) Based on Spherical MCM-41 Modified by Template Ion-Exchange in NH_3-SCR Process. *Catalysts* **2022**, *12*, 885.

(2) Lambert, C. K. Current state of the art and future needs for automotive exhaust catalysis. *Nat. Catal.* **2019**, *2*, 554−557.

(3) Liu, W.; Long, Y.; Tong, X.; Yin, Y.; Li, X.; Hu, J. Transition metals modified commercial SCR catalysts as efficient catalysts in NH_3-SCO and NH_3-SCR reactions. *Mol. Catal.* **2021**, *515*, 111888.

(4) Chang, Y.; Zou, Z.; Zhang, Y.; Deng, C.; Hu, J.; Shi, Z.; Dore, A. J.; Collett, J. L. Assessing Contributions of Agricultural and Nonagricultural Emissions to Atmospheric Ammonia in a Chinese Megacity. *Environ. Sci. Technol.* **2019**, *53*, 1822−1833.

(5) Liu, M.; Huang, X.; Song, Y.; Tang, J.; Cao, J.; Zhang, X.; Zhang, Q.; Wang, S.; Xu, T.; Kang, L.; Cai, X.; Zhang, H.; Yang, F.; Wang, H.; Yu, J. Z.; Lau, A. K. H.; He, L.; Huang, X.; Duan, L.; Ding, A.; Xue, L.; Gao, J.; Liu, B.; Zhu, T. Ammonia emission control in China would mitigate haze pollution and nitrogen deposition, but worsen acid rain. *Proc. Natl. Acad. Sci. U.S.A.* **2019**, *116*, 7760−7765.

(6) Wang, H.; Lin, M.; Murayama, T.; Feng, S.; Haruta, M.; Miura, H.; Shishido, T. Selective catalytic oxidation of ammonia to nitrogen over zeolite-supported Pt-Au catalysts: Effects of alloy formation and acid sites. *J. Catal.* **2021**, *402*, 101−113.

(7) Gao, F. Y.; Liu, Y. Y.; Sani, Z.; Tang, X. L.; Yi, H. H.; Zhao, S. Z.; Yu, Q. J.; Zhou, Y. S. Advances in selective catalytic oxidation of ammonia (NH_3-SCO) to dinitrogen in excess oxygen: A review on typical catalysts, catalytic performances and reaction mechanisms. *J. Environ. Chem. Eng.* **2021**, *9*, 104575.

(8) Sun, M.; Wang, S.; Li, Y.; Xu, H.; Chen, Y. Promotion of catalytic performance by adding W into Pt/ZrO_2 catalyst for selective catalytic oxidation of ammonia. *Appl. Surf. Sci.* **2017**, *402*, 323−329.

(9) Sun, M.; Zhou, S.; Wang, S.; Song, C. Optimized Design Method for Pt/SiO_2-Al_2O_3 with High NH_3-SCO Activity and Thermal Stability. *ACS Omega* **2022**, *7*, 3177−3184.

(10) Sun, M.; Wang, S.; Li, Y.; Wang, Q.; Xu, H.; Chen, Y. Promotion of catalytic performance by adding Cu into Pt/ZSM-5 catalyst for selective catalytic oxidation of ammonia. *J. Taiwan Inst. Chem. Eng.* **2017**, *78*, 401−408.

(11) Shrestha, S.; Harold, M. P.; Kamasamudram, K.; Kumar, A.; Olsson, L.; Leistner, K. Selective oxidation of ammonia to nitrogen on bi-functional Cu−SSZ-13 and Pt/Al_2O_3 monolith catalyst. *Catal. Today* **2016**, *267*, 130−144.

(12) Colombo, M.; Nova, I.; Tronconi, E.; Schmeißer, V.; Bandl-Konrad, B.; Zimmermann, L. Experimental and modeling study of a dual-layer (SCR+PGM) NH_3 slip monolith catalyst (ASC) for automotive SCR aftertreatment systems. *Appl. Catal. B* **2013**, *142−143*, 861−876.

(13) Lan, T. W.; Zhao, Y. F.; Deng, J.; Zhang, J. P.; Shi, L. Y.; Zhang, D. S. Selective catalytic oxidation of NH_3 over noble metal-based

catalysts: state of the art and future prospects. *Catal. Sci. Technol.* **2020**, *10*, 5792−5810.
(14) Lin, M.; An, B.; Niimi, N.; Jikihara, Y.; Nakayama, T.; Honma, T.; Takei, T.; Shishido, T.; Ishida, T.; Haruta, M.; Murayama, T. Role of the Acid Site for Selective Catalytic Oxidation of NH_3 over Au/Nb_2O_5. *ACS Catal.* **2019**, *9*, 1753−1756.
(15) Ma, H.; Schneider, W. F. Structure- and Temperature-Dependence of Pt-Catalyzed Ammonia Oxidation Rates and Selectivities. *ACS Catal.* **2019**, *9*, 2407−2414.
(16) Dann, E. K.; Gibson, E. K.; Blackmore, R. H.; Catlow, C. R. A.; Collier, P.; Chutia, A.; Erden, T. E.; Hardacre, C.; Kroner, A.; Nachtegaal, M.; Raj, A.; Rogers, S. M.; Taylor, S. F. R.; Thompson, P.; Tierney, G. F.; Zeinalipour-Yazdi, C. D.; Goguet, A.; Wells, P. P. Structural selectivity of supported Pd nanoparticles for catalytic NH_3 oxidation resolved using combined operando spectroscopy. *Nat. Catal.* **2019**, *2*, 157−163.
(17) Long, R. Q.; Yang, R. T. Superior ion-exchanged ZSM-5 catalysts for selective catalytic oxidation of ammonia to nitrogen. *Chem. Commun.* **2000**, *17*, 1651−1652.
(18) Wang, C.; Ren, D.; Harle, G.; Qin, Q.; Guo, L.; Zheng, T.; Yin, X.; Du, J.; Zhao, Y. Ammonia removal in selective catalytic oxidation: Influence of catalyst structure on the nitrogen selectivity. *J. Hazard. Mater.* **2021**, *416*, 125782.
(19) Qi, G. S.; Gatt, J. E.; Yang, R. T. Selective catalytic oxidation (SCO) of ammonia to nitrogen over Fe-exchanged zeolites prepared by sublimation of $FeCl_3$. *J. Catal.* **2004**, *226*, 120−128.
(20) Wang, F.; Zhu, Y.; Li, Z.; Shan, Y. L.; Shan, W. P.; Shi, X. Y.; Yu, Y. B.; Zhang, C. B.; Li, K.; Ning, P.; Zhang, Y.; He, H. Promoting effect of acid sites on NH_3-SCO activity with water vapor participation for Pt-Fe/ZSM-5 catalyst. *Catal. Today* **2021**, *376*, 311−317.
(21) Machida, M.; Tokudome, Y.; Maeda, A.; Sato, T.; Yoshida, H.; Ohyama, J.; Fujii, K.; Ishikawa, N. A comparative study of various transition metal overlayer catalysts for low-temperature NH_3 oxidation under dry and wet conditions. *Catal. Today* **2022**, *384*−*386*, 70−75.
(22) Górecka, S.; Pacultová, K.; Smýkalová, A.; Fridrichová, D.; Górecki, K.; Rokicińska, A.; Kuśtrowski, P.; Žebrák, R.; Obalová, L. Role of the Cu content and Ce activating effect on catalytic performance of Cu-Mg-Al and Ce/Cu-Mg-Al oxides in ammonia selective catalytic oxidation. *Appl. Surf. Sci.* **2022**, *573*, 151540.
(23) Gorecka, S.; Pacultova, K.; Fridrichova, D.; Gorecki, K.; Bilkova, T.; Zebrak, R.; Obalova, L. Catalytic Oxidation of Ammonia over Cerium-Modified Copper Aluminium Zinc Mixed Oxides. *Materials* **2021**, *14*, 6581.
(24) Amores, J. G.; Escribano, V. S.; Ramis, G.; Busca, G. An FT-IR study of ammonia adsorption and oxidation over anatase-supported metal oxides. *Appl. Catal. B.* **1997**, *13*, 45−58.
(25) Lan, T.; Deng, J.; Zhang, X.; Wang, F.; Liu, X.; Cheng, D.; Zhang, D. Unraveling the Promotion Effects of Dynamically Constructed CuO_x-OH Interfacial Sites in the Selective Catalytic Oxidation of Ammonia. *ACS Catal.* **2022**, *12*, 3955−3964.
(26) Chmielarz, L.; Jablonska, M. Advances in selective catalytic oxidation of ammonia to dinitrogen: a review. *RSC Adv.* **2015**, *5*, 43408−43431.
(27) Wang, F.; Ma, J.; He, G.; Chen, M.; Zhang, C.; He, H. Nanosize Effect of Al_2O_3 in Ag/Al_2O_3 Catalyst for the Selective Catalytic Oxidation of Ammonia. *ACS Catal.* **2018**, *8*, 2670−2682.
(28) Wang, F.; He, G.; Zhang, B.; Chen, M.; Chen, X.; Zhang, C.; He, H. Insights into the Activation Effect of H_2 Pretreatment on Ag/Al_2O_3 Catalyst for the Selective Oxidation of Ammonia. *ACS Catal.* **2019**, *9*, 1437−1445.
(29) Olofsson, G.; Hinz, A.; Andersson, A. A transient response study of the selective catalytic oxidation of ammonia to nitrogen on Pt/CuO/Al_2O_3. *Chem. Eng. Sci.* **2004**, *59*, 4113−4123.
(30) Dhillon, P. S.; Harold, M. P.; Wang, D.; Kumar, A.; Joshi, S. Y. Modeling and analysis of transport and reaction in washcoated monoliths: Cu-SSZ-13 SCR and dual-layer Cu-SSZ-13 + Pt/Al_2O_3. *ASC. React. Chem. Eng.* **2019**, *4*, 1103−1115.
(31) Ghosh, R. S.; Harold, M. P.; Wang, D. Selective oxidation of NH_3 in a Pt/Al_2O_3@Cu/ZSM-5 core-shell catalyst: Modeling and optimization. *Chem. Eng. J.* **2021**, *418*, 129065.
(32) Svintsitskiy, D. A.; Kibis, L. S.; Stadnichenko, A. I.; Slavinskaya, E. M.; Romanenko, A. V.; Fedorova, E. A.; Stonkus, O. A.; Doronkin, D. E.; Marchuk, V.; Zimina, A.; Casapu, M.; Grunwaldt, J. D.; Boronin, A. I. Insight into the Nature of Active Species of Pt/Al_2O_3 Catalysts for low Temperature NH_3 Oxidation. *Chemcatchem* **2019**, *12*, 867−880.
(33) Popa, C.; van Santen, R. A.; Jansen, A. P. J. Density-Functional Theory Study of NH_x Oxidation and Reverse Reactions on the Rh(111) Surface. *J. Phys. Chem. C* **2007**, *111*, 9839−9852.
(34) Zawadzki, J. The mechanism of ammonia oxidation and certain analogous reactions. *Discuss. Faraday Soc.* **1950**, *8*, 140−152.
(35) Zhang, L.; He, H. Mechanism of selective catalytic oxidation of ammonia to nitrogen over Ag/Al_2O_3. *J. Catal.* **2009**, *268*, 18−25.
(36) Zhang, L.; Zhang, C.; He, H. The role of silver species on Ag/Al_2O_3 catalysts for the selective catalytic oxidation of ammonia to nitrogen. *J. Catal.* **2009**, *261*, 101−109.
(37) Wang, Y.; Xu, W.; Chen, X.; Li, C.; Xie, J.; Yang, Y.; Zhu, T.; Zhang, C. Single-atom Ir_1 supported on rutile TiO_2 for excellent selective catalytic oxidation of ammonia. *J. Hazard. Mater.* **2022**, *432*, 128670.
(38) Mieher, W. D.; Ho, W. Thermally Activated Oxidation of NH_3 on Pt (111)—Intermediate Species and Reaction-Mechanisms. *Surf. Sci.* **1995**, *322*, 151−167.
(39) Sun, M.; Liu, J.; Song, C.; Ogata, Y.; Rao, H.; Zhao, X.; Xu, H.; Chen, Y. Different Reaction Mechanisms of Ammonia Oxidation Reaction on Pt/Al_2O_3 and Pt/$CeZrO_2$ with Various Pt States. *ACS Appl. Mater. Interfaces* **2019**, *11*, 23102−23111.
(40) Xu, G.; Ma, J.; Wang, L.; Xie, W.; Liu, J.; Yu, Y.; He, H. Insight into the origin of sulfur tolerance of Ag/Al_2O_3 in the H_2-C_3H_6-SCR of NOx. *Appl. Catal. B* **2019**, *244*, 909−918.
(41) Xu, G.; Ma, J.; Wang, L.; Lv, Z.; Wang, S.; Yu, Y.; He, H. Mechanism of the H_2 Effect on NH_3-Selective Catalytic Reduction over Ag/Al_2O_3: Kinetic and Diffuse Reflectance Infrared Fourier Transform Spectroscopy Studies. *ACS Catal.* **2019**, *9*, 10489−10498.
(42) Mei, D.; Kwak, J. H.; Hu, J.; Cho, S. J.; Szanyi, J.; Allard, L. F.; Peden, C. H. F. Unique Role of Anchoring Penta-Coordinated Al^{3+} Sites in the Sintering of γ-Al_2O_3-Supported Pt Catalysts. *J. Phys. Chem. Lett.* **2010**, *1*, 2688−2691.
(43) Burtin, P.; Brunelle, J. P.; Pijolat, M.; Soustelle, M. Influence of surface area and additives on the thermal stability of transition alumina catalyst supports. I: Kinetic data. *Appl. Catal.* **1987**, *34*, 225−238.
(44) Hoang, S.; Guo, Y.; Binder, A. J.; Tang, W.; et al. Activating low-temperature diesel oxidation by single-atom Pt on TiO_2 nanowire array. *Nat. Commun.* **2020**, *11* (1), 1062.
(45) Kim, M. S.; Lee, D. W.; Chung, S. H.; Hong, Y. K.; Lee, S. H.; Oh, S. H.; Cho, I. H.; Lee, K. Y. Oxidation of ammonia to nitrogen over Pt/Fe/ZSM-5 catalyst: influence of catalyst support on the low temperature activity. *J. Hazard. Mater.* **2012**, *237*−*238*, 153−160.
(46) Marceau, E.; Lauron-Pernot, H.; Che, M. Influence of the Metallic Precursor and of the Catalytic Reaction on the Activity and Evolution of Pt (Cl)/δ-Al_2O_3 Catalysts in the Total Oxidation of Methane. *J. Catal.* **2001**, *197*, 394−405.
(47) Passos, F. B.; Aranda, D. A. G.; Schmal, M. Characterization and catalytic activity of bimetallic Pt-In/Al_2O_3 and Pt-Sn/Al_2O_3 catalysts. *J. Catal.* **1998**, *178*, 478−488.
(48) Belskaya, O. B.; Leont'eva, N. N.; Zaikovskii, V. I.; Kazakov, M. O.; Likholobov, V. A. Synthesis of layered magnesium-aluminum hydroxide on the γ-Al_2O_3 surface for modifying the properties of supported platinum catalysts. *Catal. Today* **2019**, *334*, 249−257.
(49) Mang, T.; Breitscheidel, B.; Polanek, P.; Knozinger, H. Adsorption of Platinum Complexes on Silica and Alumina - Preparation of Nonuniform Metal Distributions within Support Pellets. *Appl. Catal. A* **1993**, *106*, 239−258.

https://doi.org/10.1021/acsomega.3c00381
ACS Omega 2023, 8, 13944−13954

(50) Wang, Y.; Xu, W.; Li, C.; Yang, Y.; Geng, Z.; Zhu, T. Effects of IrO_2 nanoparticle sizes on Ir/Al_2O_3 catalysts for the selective catalytic oxidation of ammonia. *Chem. Eng. J.* **2022**, *437*, 135398.
(51) Peng, P.; Li, J.; Mo, S.; Zhang, Q.; Shen, T.; Xie, Q. Bimetallic Pt-Co Nanoparticle Deposited on Alumina for Simultaneous CO and Toluene Oxidation in the Presence of Moisture. *Processes* **2021**, *9*, 230.
(52) Jan, A.; Shin, J.; Ahn, J.; Yang, S.; Yoon, K. J.; Son, J. W.; Kim, H.; Lee, J. H.; Ji, H. I. Promotion of Pt/CeO_2 catalyst by hydrogen treatment for low-temperature CO oxidation. *RSC Adv.* **2019**, *9*, 27002−27012.
(53) Cant, N. W.; Little, L. H. Lewis and Bronsted Acid Sites on Silica-Alumina. *Nature* **1966**, *211*, 69−70.
(54) Bahrami, B.; Komvokis, V. G.; Singh, U. G.; Ziebarth, M. S.; Alexeev, O. S.; Amiridis, M. D. In situ FTIR characterization of NH_3 adsorption and reaction with O_2 and CO on Pd-based FCC emission control additives. *Appl. Catal. A-Gen.* **2011**, *391*, 11−21.
(55) Lin, S. D.; Gluhoi, A. C.; Nieuwenhuys, B. E. Ammonia oxidation over $Au/MO/\gamma\text{-}Al_2O_3$—activity, selectivity and FTIR measurements. *Catal. Today* **2004**, *90*, 3−14.
(56) Xu, G.; Zhang, Y.; Lin, J.; Wang, Y.; Shi, X.; Yu, Y.; He, H. Unraveling the Mechanism of Ammonia Selective Catalytic Oxidation on Ag/Al_2O_3 Catalysts by Operando Spectroscopy. *ACS Catal.* **2021**, *11*, 5506−5516.
(57) Dai, Q.; Zhu, Q.; Lou, Y.; Wang, X. Role of Brønsted acid site during catalytic combustion of methane over PdO/ZSM-5: Dominant or negligible? *J. Catal.* **2018**, *357*, 29−40.
(58) Manjunathan, P.; Prasanna, V.; Shanbhag, G. V. Exploring tailor-made Brønsted acid sites in mesopores of tin oxide catalyst for β-alkoxy alcohol and amino alcohol syntheses. *Sci. Rep.* **2021**, *11*, 15718.
(59) Kamata, H.; Takahashi, K.; Odenbrand, C. I. Surface acid property and its relation to SCR activity of phosphorus added to commercial $V_2O_5(WO_3)/TiO_2$ catalyst. *Catal. Lett.* **1998**, *53*, 65−71.
(60) Pang, C.; Han, R.; Su, Y.; Zheng, Y.; Peng, M.; Liu, Q. Effect of the acid site in the catalytic degradation of volatile organic compounds: A review. *Chem. Eng. J.* **2023**, *454*, 140125.
(61) Savva, P.; Efstathiou, A. The influence of reaction temperature on the chemical structure and surface concentration of active NOx in H_2-SCR over $Pt/MgO\text{-}CeO_2$: SSITKA-DRIFTS and transient mass spectrometry studies. *J. Catal.* **2008**, *257*, 324−333.
(62) Hadjiivanov, K. I. Identification of Neutral and Charged N_xO_ySurface Species by IR Spectroscopy. *Catal. Rev.* **2000**, *42*, 71−144.
(63) Szanyi, J.; Kwak, J. H.; Chimentao, R. J.; Peden, C. H. F. Effect of H_2O on the Adsorption of NO_2 on $\gamma\text{-}Al_2O_3$: an in Situ FTIR/MS Study. *J. Phys. Chem. C* **2007**, *111*, 2661−2669.
(64) Zhanpeisov, N. U.; Martra, G.; Ju, W. S.; Matsuoka, M.; Coluccia, S.; Anpo, M. Interaction of N_2O with Ag^+ ion-exchanged zeolites: an FT-IR spectroscopy and quantum chemical ab initio and DFT studies. *J. Mol. Catal. A-Chem.* **2003**, *201*, 237−246.
(65) Ramis, G.; Angeles Larrubia, M. An FT-IR study of the adsorption and oxidation of N-containing compounds over Fe_2O_3/Al_2O_3 SCR catalysts. *J. Mol. Catal. A: Chem.* **2004**, *215*, 161−167.
(66) Scheuer, A.; Hauptmann, W.; Drochner, A.; Gieshoff, J.; Vogel, H.; Votsmeier, M. Dual layer automotive ammonia oxidation catalysts: Experiments and computer simulation. *Appl. Catal. B: Environ.* **2012**, *111−112*, 445−455.
(67) Machida, M.; Tokudome, Y.; Maeda, A.; Kuzuhara, Y.; Hirakawa, T.; Sato, T.; Yoshida, H.; Ohyama, J.; Fujii, K.; Ishikawa, N. Nanometric Platinum Overlayer to Catalyze NH_3 Oxidation with High Turnover Frequency. *ACS Catal.* **2020**, *10*, 4677−4685.
(68) Xu, G.; Li, H.; Yu, Y.; He, H. Dynamic Change of Active Sites of Supported Vanadia Catalysts for Selective Catalytic Reduction of Nitrogen Oxides. *Environ. Sci. Technol.* **2022**, *56*, 3710−3718.
(69) Ungerer, M. J.; Santos-Carballal, D.; Cadi-Essadek, A.; van Sittert, C. G. C. E.; de Leeuw, N. H. Interaction of H_2O with the Platinum Pt (001), (011), and (111) Surfaces: A Density Functional Theory Study with Long-Range Dispersion Corrections. *J. Phys. Chem. C* **2019**, *123*, 27465−27476.
(70) Jalilehvand, F.; Laffin, L. J. Structure of the Hydrated Platinum(II) Ion and the cis-Diammineplatinum(II) Complex in Acidic Aqueous Solution: An EXAFS Study. *Inorg. Chem.* **2008**, *47*, 3248−3254.

https://doi.org/10.1021/acsomega.3c00381
ACS Omega 2023, 8, 13944−13954